

1. Introduction

One of the key information needs for performance assessment of a potential high-level nuclear waste repository at Yucca Mountain, Nevada, is the quantification of ground-water infiltration and travel times in the unsaturated zone. Related to this need is the identification of fast fluid pathways – features such as faults and fractures through which infiltrating water may partly bypass the rock matrix. These needs are being addressed in part by ^{36}Cl isotopic studies of surface samples, drill cores and cuttings, and, most recently, samples from the Exploratory Studies Facility (ESF) (Fig. 1). The isotopic studies are fully integrated with mineralogic and textural analysis of transmissive features as well as with numerical modeling of ground-water infiltration (Fabryka-Martin et al., in press).

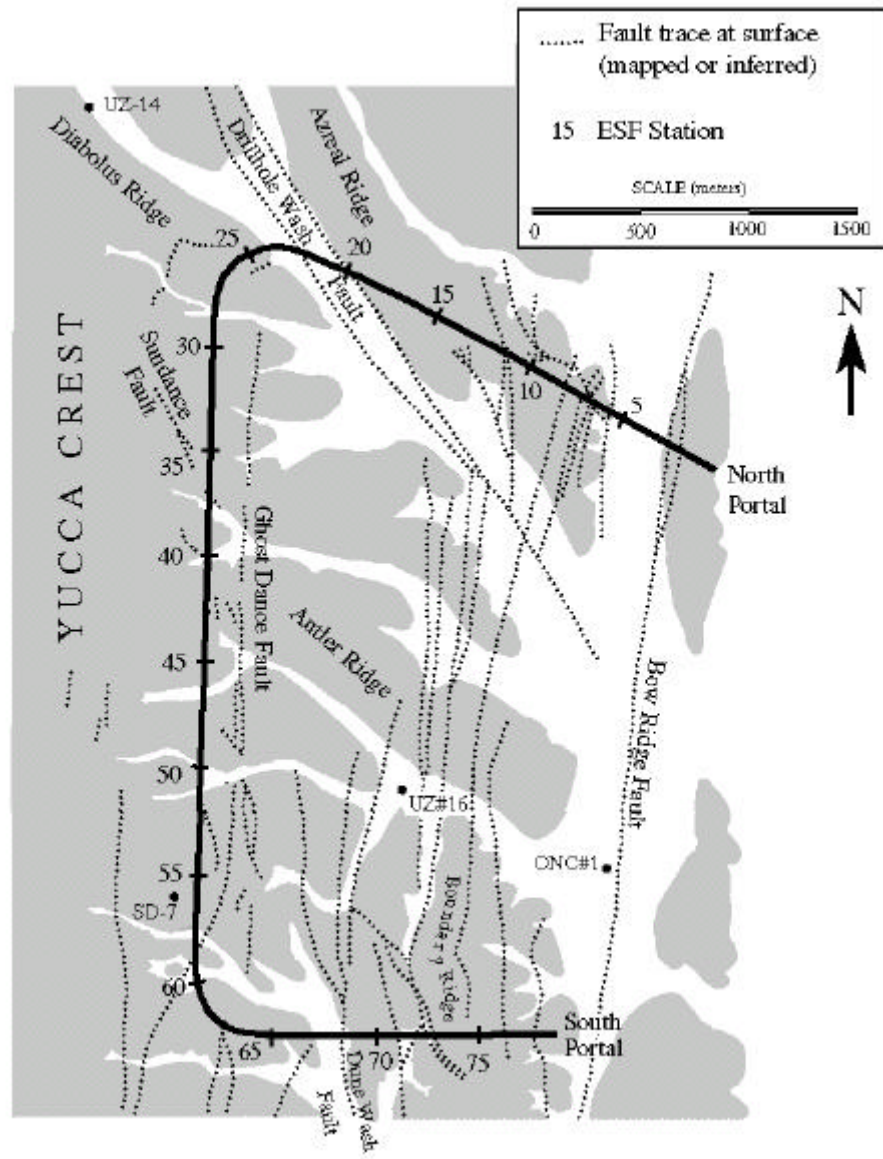


Figure 1. Plan view of ESF tunnel, showing its relationship to selected boreholes and faults mapped at the surface. The ESF tunnel was completed to Station 77 when this report was prepared. Location of faults is based on Day et al. (1996); not all faults on that map are shown here. See Day et al. for the distinction between faults that are mapped as opposed to those which are inferred.

The ESF is an ~8-m-diameter tunnel beneath Yucca Mountain, extending as deep as the potential repository level. When completed, it will be 8.0 km long. In contrast with drill-hole studies, examination of the tunnel exposures allows detailed characterization of the petrologic and structural settings of sample sites. The silicic tuffs exposed in the ESF include three main stratigraphic units of the Miocene Paintbrush Group (Sawyer et al., 1994): the mostly welded Tiva Canyon Tuff, an underlying interval of variably welded pyroclastic deposits, and the mostly welded Topopah Spring Tuff, in order of increasing age and depth. The stratigraphic interval within the Paintbrush Group at Yucca Mountain that extends from the base of the densely welded and devitrified portion of the Tiva Canyon Tuff downward to the top of the densely welded portion of the underlying Topopah Spring Tuff corresponds to the PTn hydrologic unit (Montazer and Wilson, 1984; Ortiz et al., 1985), used in modeling efforts. This interval includes parts or all of four formations (the Tiva Canyon Tuff, the Yucca Mountain Tuff, the Pah Canyon Tuff, and the Topopah Spring Tuff) and three informally designated intervening bedded tuff units (Moyer et al., 1996).

Chlorine-36 investigations are part of an extensive hydrologic testing program in the ESF. The use of ^{36}Cl as a tracer and as a means of dating ground water is based on the production of this cosmogenic isotope in the atmosphere and its incorporation into infiltrating water. Once isolated from the atmosphere, the ^{36}Cl content of the ground water gradually decreases as a result of radioactive decay with a half-life of 301,000 yr. Chloride (Cl) extracted from the accessible pore spaces of subsurface samples is representative of the water that moved through the rock. Water ages, representing estimates of ground-water travel time from the surface to the underground sample sites, may be calculated from the decay constant for ^{36}Cl , the sample $^{36}\text{Cl}/\text{Cl}$, the initial meteoric $^{36}\text{Cl}/\text{Cl}$, and the secular equilibrium $^{36}\text{Cl}/\text{Cl}$ produced by the *in situ* subsurface neutron flux from the decay of natural uranium and thorium isotopes in the rock (Fabryka-Martin et al., in press).

An additional hydrologic application of ^{36}Cl , and the focus of the studies reported here, is the input of anthropogenic ^{36}Cl into the ground-water system. Waters entering the subsurface during the last 40 years contain high concentrations of ^{36}Cl relative to natural background values. The elevated values are traceable to global fallout from more than 70 atmospheric nuclear tests conducted between 1952 and 1958 (Glasstone, 1962). This input provides a fortuitous tracer to identify very young infiltrating water. ESF samples with $^{36}\text{Cl}/\text{Cl}$ values indicating a component of bomb-pulse ^{36}Cl are the basis for identifying fast pathways in the subsurface.

In the data set of Fabryka-Martin et al. (in press), which reported ^{36}Cl results available as of August 1996, fourteen samples (13%) have corrected $^{36}\text{Cl}/\text{Cl}$ ratios less than the present-day background value of 500×10^{-15} , whereas 60 samples (57%) have values between 500×10^{-15} and 1250×10^{-15} . This is the range over which the atmospheric $^{36}\text{Cl}/\text{Cl}$ ratio has varied prior to the introduction of bomb-pulse ^{36}Cl from above-ground nuclear testing. Thirty-one samples (30%) have ratios above 1250×10^{-15} ; these are primarily from faults, fractures, or breccia zones. The working hypothesis presented in Fabryka-Martin et al. (in press) is that samples with $^{36}\text{Cl}/\text{Cl}$ ratios above 1250×10^{-15} contain a component of bomb-pulse ^{36}Cl and therefore indicate the presence of water less than 40 years old.

Numerical modeling efforts are under way to simulate Cl transport in the unsaturated zone at Yucca Mountain, with a specific emphasis on interpretation and analysis of $^{36}\text{Cl}/\text{Cl}$ values in the ESF. One part of the modeling effort is an investigation of the combinations of net infiltration and rock hydrologic properties that result in the arrival of at least a small amount of water with the bomb-pulse signature at the middle nonlithophysal zone of the Topopah Spring Tuff (main drift of the ESF) in 40 years or less. Results indicate that the hydraulic conductivity of the PTn hydrologic unit is the key parameter controlling ground-water travel time to the ESF level. Simulations utilizing the "base-case" hydrologic properties for the PTn described by Fabryka-Martin et al. (in press) do not result in the arrival of bomb-pulse ^{36}Cl at the ESF within the necessary time interval, even for infiltration rates as high as 50 mm/yr. Faults in the PTn were simulated by increasing fracture frequency and apertures above "base-case" values; with this increased permeability, infiltration rates of 1 to 5 mm/yr were found to be sufficient to transport small amounts of bomb-pulse ^{36}Cl to the ESF level within 40 years.

The simulations support the hypothesis that bomb-pulse ^{36}Cl arrived in the ESF by way of pathways connected to faults or other features of increased fracture permeability in the PTn. This outcome is compatible in a general sense with field observations that many bomb-pulse sites are close to fault zones that are thought to be correlative with faults mapped at the surface (Barr et al., 1996; Day et al., 1996). The properties of the actual transmissive structures have not yet been explicitly incorporated into numerical models because the necessary information is still being collected and analyzed.

This report updates the data base of ^{36}Cl measurements of ESF samples and describes our progress in developing conceptual models for different types of fast pathways:

- Section 2 summarizes the analytical methods used to collect and analyze samples for isotopic and mineralogic characteristics, and the guidelines used for descriptions of structural features in the field.
- Section 3 updates the data base of ^{36}Cl results and subjects them to statistical analysis to provide a basis for identifying those samples which contain a component of bomb-pulse ^{36}Cl , an indicator of a fast transport path from the surface to the sample location. Results of paired analyses of fine-grained breccia and associated broken rock appear to have implications for the extent of matrix-fracture interactions.
- Sections 4 and 5 provide brief overviews of the major tectonic structures and the smaller-scale fracture networks at Yucca Mountain, focusing on the manner in which these structural features establish a framework for flow paths.
- Section 6 proposes that the distribution of fast paths in the ESF is governed by three necessary conditions, a conceptual model that is supported by case studies.
- Section 7 provides an overview of the origin and timing of fracture mineral coatings and examines the extent to which these minerals may provide a guide to the recognition of fast paths.

The present report is a mid-year progress report outlining the basic ideas of the structural controls and mineralogic associations of fast paths. Section 8 emphasizes the aspects of this analysis of fast paths on which our work will continue to focus in the upcoming months, culminating in the development of a conceptual model of fast-path distribution at Yucca Mountain, and recommendations as to how this model can be incorporated into site-scale flow and transport models.

2. Analytical Methods

2.1. Sample Collection

Geologic samples in the ESF were selected for ^{36}Cl analysis to provide a systematic representation of the bedrock and to include likely transmissive features such as faults, fractures, and breccia zones. Samples collected as of March 1997 are listed in Appendix A, along with their locations and general characteristics. ESF sample locations are measured inward from the north portal. For example, a location 115 m inward is designated as Station (abbreviated Sta.) 1+15 (Fig. 1). Bedrock samples were collected at 200-m intervals along the tunnel between Sta. 5 and 61, and at 100-m intervals between Sta. 61 and 69. In addition, a large variety of features was sampled to test for the existence of fast fluid pathways. Multiple samples were collected at several locations to obtain information about the distribution of ^{36}Cl within fault/breccia zones or between highly fractured rock and adjacent, less-fractured bedrock. Depths from the ground surface to the ESF range from about 40 m at Sta. 2 to about 300 m at Sta. 34.

2.2. Mineralogic and Petrologic Analysis

Subsamples designated for mineralogic and petrologic study were examined by binocular microscope. Contamination of the rock materials by Cl was avoided by the use of new examination gloves for each sample. Mineral identifications are based on color, morphology, hardness, comparison to known materials, limited X-ray diffraction analysis, and evidence of fluorescence under ultraviolet light. Some ambiguities of mineral identification are unresolved; for example, clay and mordenite (a zeolite) in minute deposits cannot be distinguished without electron microscopy or similar techniques. Standard color charts were not used to determine color names because they are a potential source of Cl cross-contamination.

X-ray powder diffraction data for selected samples were obtained on an automated Siemens D-500 diffractometer using Cu-K α radiation, incident- and diffracted-beam Soller slits, and a Kevex (SiLi) solid-state detector. Data were collected from 2 to 50° 2 θ and count times ≥ 2.0 s per step. Quantitative analyses employed the internal standard method of Chung (1974a,b) using 1.0- μm corundum as the internal standard.

2.3. Chlorine Isotopic Analysis

Chloride was extracted from one- to five-kg rock samples by leaching them with an equal mass of deionized water for 48 hours. The Cl of interest is on the outer surfaces of particles or fractures. Poorly cohesive material was leached without further comminution, but other samples were generally crushed to 1- to 2-cm size fragments prior to leaching in order to increase the efficiency of extracting porewater salts. An aliquot of the leachate was analyzed for

Cl and Br by ion chromatography to estimate the contribution of Cl from construction water traced with lithium bromide (LiBr). The remaining leachate was decanted, acidified to promote settling of particulates, and filtered. Known quantities of isotopically pure ^{35}Cl were added to samples with total Cl concentrations less than 2 mg. Silver nitrate was added to the leachates to precipitate silver chloride, AgCl. The AgCl was purified of sulfur, which has an interfering isobar at mass 36, by multiple cycles of dissolution in ammonium hydroxide with addition of barium nitrate to precipitate barium sulfate, followed by reprecipitation of the AgCl with nitric acid. The purified AgCl precipitates were sent to the Purdue Rare Isotope Measurement (PRIME) Laboratory for Cl isotopic analysis by accelerator mass spectrometry.

Based on Br/Cl ratios in the salts leached from the rocks, measured $^{36}\text{Cl}/\text{Cl}$ ratios are adjusted for the presence of Cl from construction water, which has been isotopically characterized and labeled with LiBr (Fabryka-Martin et al., in press). It is important to note that, because the $^{36}\text{Cl}/\text{Cl}$ ratio of the construction water (500×10^{-15}) is equal to the present-day (pre-bomb) background $^{36}\text{Cl}/\text{Cl}$ level, ^{36}Cl levels above present-day background cannot be attributed to this source. The corrected ratios are presented in Appendix B and discussed in Section 3. All equipment is checked routinely for contamination through the frequent analysis of process blanks.

2.4. Structural Analysis

Structural investigations have been conducted in order to evaluate the structural significance and characterize the possible hydrologic pathways exploited by water that has transmitted bomb-pulse ^{36}Cl to sample locations in the North Ramp and Main Drift of the ESF. The methodology for evaluating the ^{36}Cl results involves combining a) surface and subsurface structural features; b) vertical connectivity and characteristics of the fractures and fracture network(s) in the TCw (welded part of the Tiva Canyon Tuff), the PTn, and TSw (welded part of the Topopah Spring Tuff) units; and c) possible changes in fracture intensity near fault zones. Surface geologic mapping, full-periphery mapping in the ESF and detailed line survey data in the ESF are being digitally integrated to evaluate structural controls of ^{36}Cl distribution. Observations being collected at each sample locality include: description of the sampled feature (orientation, length, aperture, interpreted origin), local structural setting (fracture set interpretation, location with respect to known faults), and interpreted connection to other features.

2.5. Recognition of Syngenetic Features

The identification of transmissive features of syngenetic origin is an important aspect of sampling site characterization. Syngenetic features are formed during the cooling of a newly emplaced ash flow. A syngenetic origin of fractures or breccia zones carries useful implications of age and spatial continuity. Cooling joints, in particular, do not extend beyond the boundaries of an ash flow into underlying or overlying units. Their extent may be further limited by changes in syngenetic textural zonation; for example, cooling joints may be well developed in densely welded, nonlithophysal tuff but die out across a transition into lithophysal tuff where thermal contraction was accommodated by mechanisms other than tensile fracturing. These limitations of spatial continuity imply that transmissive features of purely syngenetic origin can be fast pathways only if they are connected to throughgoing pathways such as faults. In some cases, post-emplacement tectonic deformation can exploit the pre-existing fractures and breccias, creating pathways of hybrid origin (Potter et al., 1996b; Sweetkind et al., 1996b).

Significant syngenetic features for the study of fast paths include vapor-phase partings, cooling joints, syngenetic fractures, and syngenetic breccias. Vapor-phase partings are discontinuous, incipient fractures with fillings of mostly high-temperature silica minerals and feldspar. The partings commonly formed subparallel to flattening foliation. Cooling joints typically have low surface roughness and are planar to arcuate. Distinctive light-colored margins as much as a few millimeters thick, also known as "bleached margins," are common attributes of cooling joints. Breccias and fractures other than cooling joints may be identifiable as syngenetic by the presence of certain mineral cements and fracture fillings. Tridymite, cristobalite, and alkali feldspar deposits are highly reliable indicators that fractures or breccias formed early in the cooling history of an ash flow; euhedral quartz and chalcedony are deposited later in the cooling history at near-ambient temperatures (Levy, 1993; Levy and O'Neil, 1989).

3. Chlorine-36 Analyses in the ESF

3.1. Analytical Results

The last progress report for the Water Movement Test activity (Fabryka-Martin et al., in press) covered sample collection as far as Sta. 56+93 and reported analytical data to Sta. 45+79. As of March 1997, sampling to Sta. 69+42 has been accomplished and 189 analyses are available for 173 sample locations up to Sta. 67+90 (Appendix

B). About 70% of the analyses are for samples collected from faults, fractures, lithophysal cavities, breccia zones, and broken rock. Thirty-three systematic samples compose 17% of the analytical data base, and the remaining 12% of the analyses (22 samples) are subunit contacts in and above the PTn unit. Analyses for many of these samples were reported previously in Fabryka-Martin et al. (in press) and Levy et al. (in press); differences in the two sets of reported values are attributable to recent changes in the error estimation protocol used by the analytical laboratory, and to reanalysis of selected samples to improve analytical precision.

The results are plotted as a function of distance into the ESF tunnel in Fig. 2. The data fall clearly into two distinct populations, as can be seen also in a frequency histogram plot (Fig. 3). The majority of the samples have corrected $^{36}\text{Cl}/\text{Cl}$ ratios ranging between 300×10^{-15} and 1200×10^{-15} , or 0.6 to 2.4 times the present-day background value of 500×10^{-15} . These results fall well within the range over which the atmospheric $^{36}\text{Cl}/\text{Cl}$ signal has varied during the past 50 ky or more (Fabryka-Martin et al., in press). However, at a few locations, ratios extend well above this range, to a maximum of 4100×10^{-15} . These high ratios are interpreted as indicating the presence of a component of bomb-pulse ^{36}Cl at these locations. Zones in which multiple samples show indications of bomb-pulse ^{36}Cl appear to be associated with faults mapped at the surface. No samples containing unambiguous levels of bomb-pulse ^{36}Cl have yet been detected in any of the 53 samples analyzed beyond Sta. 45.

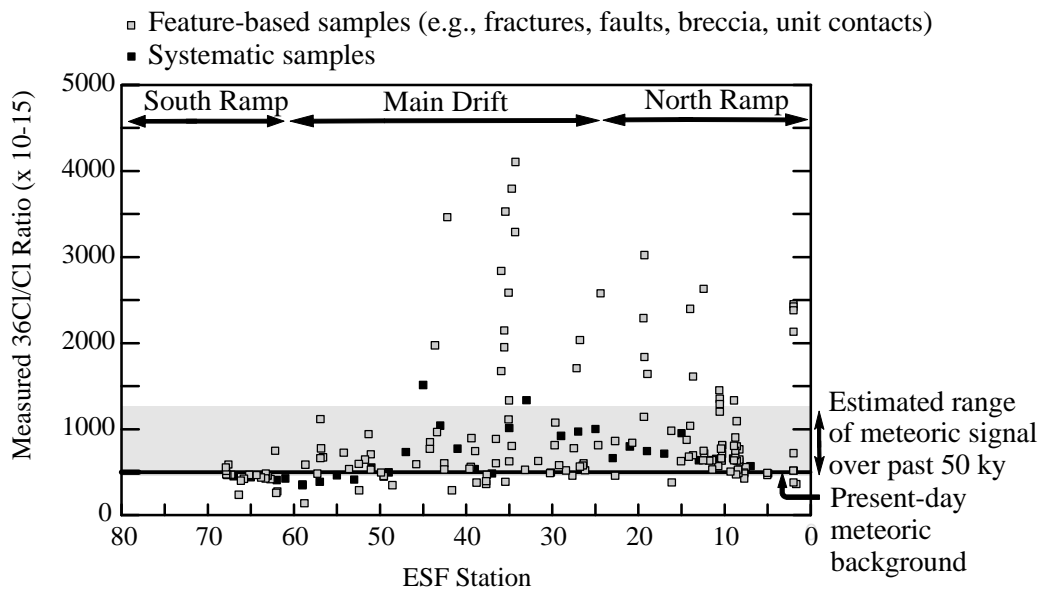


Figure 2. Distribution of $^{36}\text{Cl}/\text{Cl}$ ratios measured for rock samples, as a function of distance along the ESF as measured from the North Ramp Portal. ESF stations are marked 100-m increments. Samples with ratios exceeding 1250×10^{-15} are considered to contain a component of bomb-pulse ^{36}Cl . Data from Appendix B.

3.2. Statistical Analysis of Chlorine-36 Data

Chauvenet's criterion for identifying outliers is the basis of the statistical test used to establish the cutoff ratio above which a sample result is considered to be elevated above natural background (Bevington and Robinson, 1992). The approach taken in this report is to rank the 189 data points (Appendix B) from lowest to highest value, and to calculate a cumulative average and standard deviation for each step of the ranking. One then calculates the number of standard deviations that the highest-value data point lies above the mean as each new data point is included in the cumulative average. These standard deviations are plotted in Fig. 4, in which they are compared against Chauvenet's criterion for identifying outliers (solid line) as a function of ranking. This criterion states that a data point is an outlier of a Gaussian (normal) distribution if the probability of such a value being that far from the cumulative mean of the ranked data set is less than 0.5% (Bevington and Robinson, 1992).

The plot of sample standard deviations versus sample rank (Fig. 4) varies smoothly within the region of background values but shows an abrupt jump between samples ranked 157 and 158, $^{36}\text{Cl}/\text{Cl}$ ratios of 1202×10^{-15} and 1292×10^{-15} for samples E196-2 and E195-2, respectively. For the latter sample, the calculated number of standard deviations exceeds Chauvenet's criterion for identifying statistical outliers. Hence, all subsequent values above that measured for E196-2 are also considered to lie outside the range of the population of background samples. The cutoff value is a ratio of about 1250×10^{-15} , although the value might shift slightly in the future as more data are obtained. In the histogram plot of Fig. 3, this value also marks the upper limit of the normal distribution of the background samples. Figure 3 shows that the background data do not follow a truly Gaussian distribution but rather are moderately skewed, with a Pearson coefficient of skewness of 0.57. However, this deviation from ideal conditions does not significantly affect the test results. Another indication that the statistically-based cutoff value is reasonable is its consistency with the maximum background ratio determined from analyses of 31 packrat midden samples from southern Nevada (Fabryka-Martin et al., in press). These samples track variations in the atmospheric $^{36}\text{Cl}/\text{Cl}$ ratio. The highest ratio in this data set, $1270 \pm 90 \times 10^{-15}$, was obtained for a midden sample dated at 12.35 ky by the carbon-14 method.

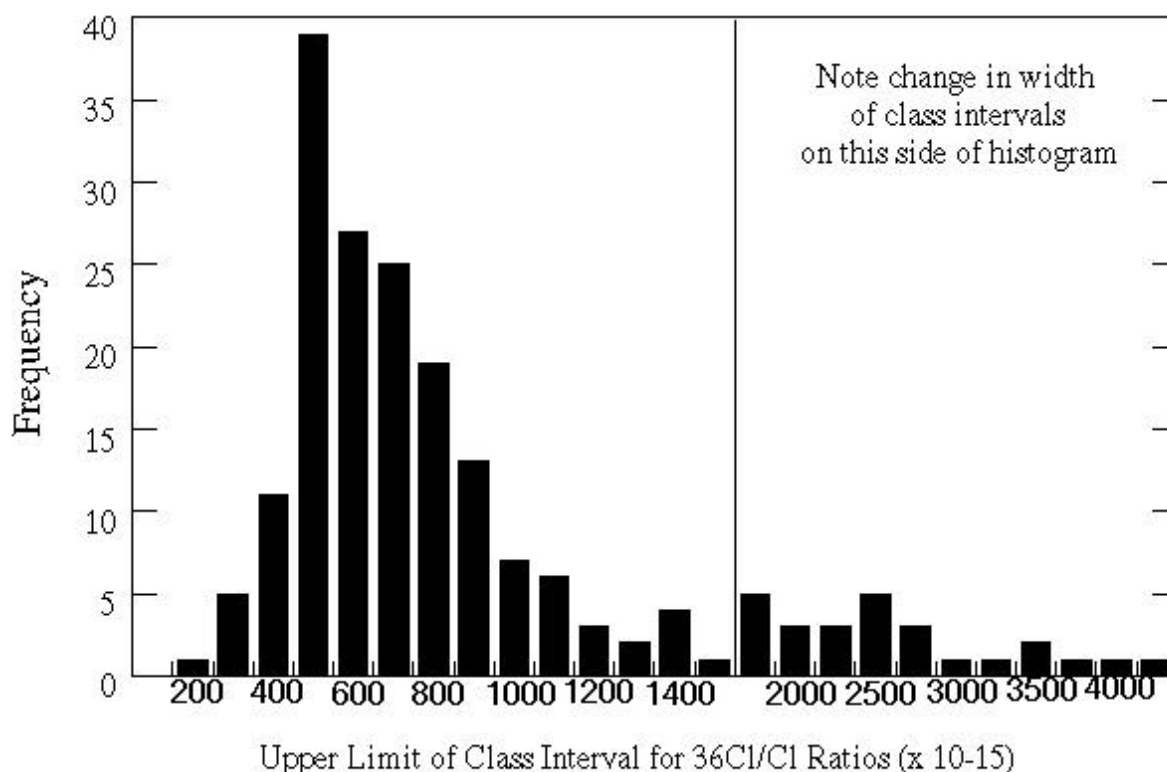


Figure 3. Frequency distribution of $^{36}\text{Cl}/\text{Cl}$ ratios measured in ESF rock samples. Data from Appendix B.

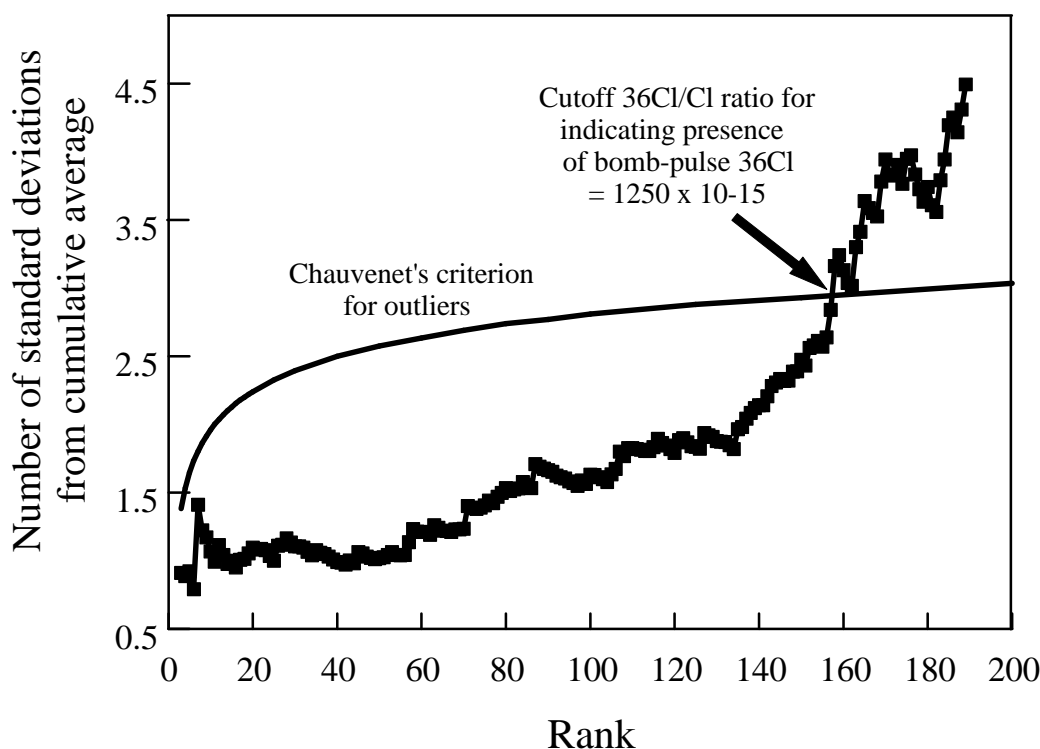


Figure 4. Application of Chauvenet's criterion to establish the cutoff $^{36}\text{Cl}/\text{Cl}$ ratio for identifying the presence of bomb-pulse ^{36}Cl in ESF rock samples. See section 3.2 for discussion of this approach. Data from Appendix B.

In summary, based on Chauvenet's criterion, a sample with a $^{36}\text{Cl}/\text{Cl}$ ratio significantly higher than a cutoff of 1250×10^{-15} is interpreted as being clearly elevated above meteoric background and most likely contains a component of bomb-pulse ^{36}Cl . Samples with ratios higher than the present-day value of 500×10^{-15} but less than 1250×10^{-15} may also contain a component of bomb-pulse ^{36}Cl but may also contain Cl from water recharged during a time when the input ratio was higher than the present-day value (Fabryka-Martin et al., in press).

3.3. Paired Analyses of Coarse and Fine Breccia Materials and Rock Fragments

The kilogram-size samples required for isotopic analysis preclude our investigating the fine-scale spatial distribution of bomb-pulse ^{36}Cl within samples. A preliminary attempt was made to detect differences related to fragment size in breccia samples as a possible indicator of matrix/fracture interactions. Six breccia samples from Sta. 13 to 37 which had been collected into single sample bags were manually sifted in the laboratory into separates with particle sizes either larger or smaller than ~ 0.5 cm. The finer fractions were processed for analysis without further size reduction. For the coarser fractions, the larger rock fragments were individually crushed with a steel plate and hammer to a maximum size of ~ 2 cm, then processed for analysis. Six additional samples from Sta. 34 to 59 consisted of breccia and the adjacent rock or cooling joint surface collected into separate bags. These texturally distinct materials were processed and analyzed separately.

The choice of 0.5 cm as the criterion for separating breccia samples into coarse and fine fractions does not result in the production of separates with any true genetic significance because it does not consistently separate "wall rock" from "fault gouge" or "broken but intact rock" from "mineralogically altered gouge" or "bedrock fragments" from "cement." Despite this cautionary note, the paired analyses of coarse and fine fractions or of broken wall rock and adjacent breccia from Stations 13+67 through 35+93 show a consistent pattern of higher $^{36}\text{Cl}/\text{Cl}$ values in the coarse fractions (Fig. 5). All of the coarse-fraction values and about half the fine-fraction values in this interval are above

the bomb-pulse threshold. Samples from Sta. 36+55 and beyond have lower, non-bomb-pulse values and generally smaller differences between size separates.

Petrologic and mineralogic examination of the analyzed separates remains to be done, but a few generalized observations may be relevant to the isotopic results. The baseline interpretation supported by the results from Stations 13+67 through 35+93 is that the accessible pore spaces of the fast fluid pathways are not in equilibrium with respect to the ^{36}Cl isotopic signal. Because these samples all represent active fast pathways that have apparently received infiltration from the surface within the past forty years, and because the isotopic composition of the infiltration they receive has changed significantly over this short period due to input of bomb-pulse ^{36}Cl , isotopic disequilibrium within the fluid pathway is readily detectable. In areas of the ESF where ground-water travel times are apparently on the order of tens to hundreds of thousands of years or more, the changes of isotopic composition in the infiltrating water moving through these rocks probably occurred so gradually over this period that a lack of isotopic equilibrium between matrix and fracture porewater would not be detectable by a comparison of their ^{36}Cl signals.

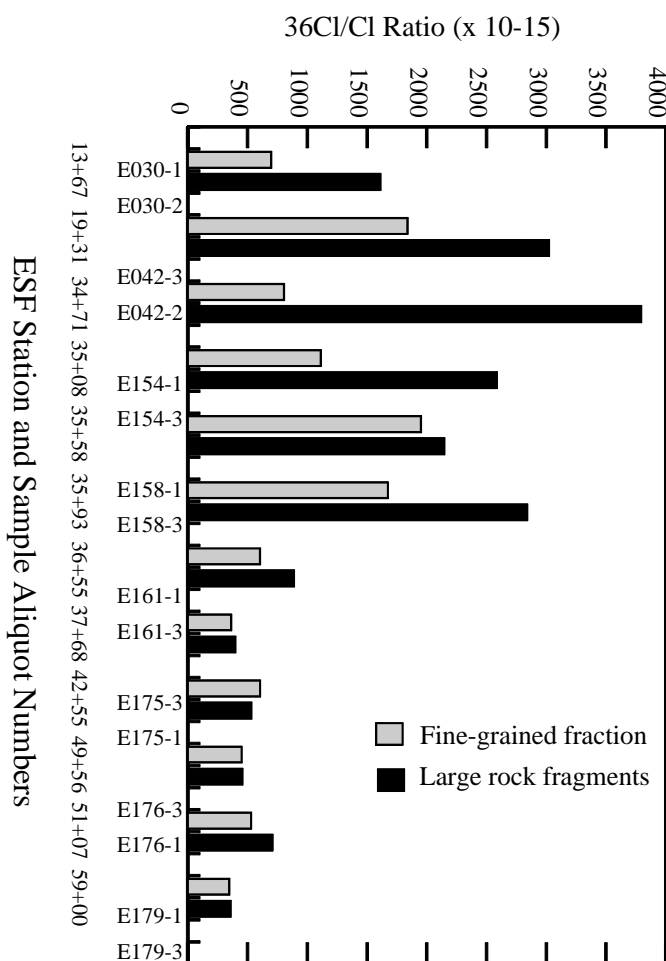


Figure 5. Analytical results for paired size separates. Each pair was collected at a single location. At some locations, a single sample was collected and manually separated in the laboratory into coarse and fine subsamples. Elsewhere, the different size separates were collected separately in the field to be representative of the fault or fracture infilling and of the adjacent wallrock. Site descriptions in Appendix A, and data from Appendix B.